

MASS TRANSFER IN CLOSE, RAPIDLY ACCRETING PROTOBINARIES: AN ORIGIN FOR MASSIVE TWINS?

MARK R. KRUMHOLZ* AND TODD A. THOMPSON†

Department of Astrophysical Sciences, Princeton University, Princeton, NJ 08544

Submitted to the Astrophysical Journal, November 22, 2006

ABSTRACT

Rapidly accreting massive protostars undergo a phase of deuterium shell burning during pre-main sequence evolution that causes them to swell to tenths of an AU in radius. During this phase, those with close binary companions will overflow their Roche lobes and begin transferring mass. Since massive stars frequently have companions at distances well under 1 AU, this process may affect the early evolution of a substantial fraction of massive stars. We use a simple protostellar evolution model to determine the range in accretion rates, mass ratios, and orbital separations for which mass transfer will occur, and we compute approximately the stability and final outcome of the transfer process. We discuss how mass transfer affects the demographics of massive binaries, and show that it provides a natural explanation for the heretofore unexplained population of massive “twins”, high mass binaries with mass ratios very close to unity.

Subject headings: accretion, accretion disks — binaries: close — binaries: spectroscopic — stars: evolution — stars: formation — stars: pre-main sequence

1. INTRODUCTION

Massive stars form in regions of high pressure and density that produce high accretion rates. Simple order-of-magnitude estimates for the properties of observed massive protostellar cores suggest that accretion rates of $\sim 10^{-4} - 10^{-2} M_{\odot} \text{ yr}^{-1}$ are typical (Krumholz 2006), and both detailed analytic models (McKee & Tan 2003) and numerical simulations (Krumholz et al. 2007) produce accretion rates in this range. Observations of protostellar outflows with mass fluxes up to $\sim 10^{-2} M_{\odot} \text{ yr}^{-1}$ from luminous embedded protostars (Henning et al. 2000) also suggest high accretion rates.

The combination of rapid accretion and high mass produces protostars with very large radii, for two reasons. First, Stahler (1988) shows that prior to the onset of deuterium burning, the radius of an accreting protostar is determined primarily by the specific entropy of the gas after it passes through the accretion shock, radiates and settles onto the surface, and is eventually buried in enough optical depth to prevent it from radiating further. A high accretion rate reduces the amount of time an accreted gas element has to radiate before it is buried, and thus produces higher specific entropy and larger radius. Second, Palla & Stahler (1991, 1992) show that after deuterium burning begins, massive protostars pass through a period of shell burning. This occurs because, as contraction raises the core temperature, the opacity decreases to the point where a convectively stable layer forms. Accreting deuterium cannot pass through this radiative barrier to reach the core. As a result, deuterium burning occurs in a shell around the core, which, in a process analogous to that in a red giant, produces rapid expansion of the envelope above the burning layer. Together, these two effects can produce radii of several tenths an AU during pre-main sequence evolution of

rapidly accreting stars.

Large radii create the possibility for mass transfer in close binaries. Most massive stars appear to be in multiple systems (e.g. Preibisch et al. 2001; Shatsky & Tokovinin 2002; Lada 2006). While the semi-major axis distribution of massive stars is not well-determined, due to low statistics and complex selection biases, there appears to be a significant population of very close binaries. The WR20a system, the most massive binary known, has a separation of only 0.25 AU (Bonanos et al. 2004; Rauw et al. 2005). The semi-major axis of the massive detached eclipsing binary D33J013346.2+304439.9 in M33 is 0.22 AU (Bonanos et al. 2006). Harries et al. (2003) and Hilditch et al. (2005) report a sample of 50 OB star eclipsing binaries with periods of 5 days or less taken from the Optical Gravitational Lens Experiment survey (OGLE; Udalski et al. 1998) of the SMC. This corresponds to a semi-major axis of $0.26 M_{100}^{1/3}$ AU, where M_{100} is the total mass in units of $100 M_{\odot}$. Roughly half the systems are detached binaries, indicating that they have not yet undergone any post-main sequence mass transfer. It is therefore likely that these systems formed at close to their current separations, or possibly even closer, since mass loss from winds during main sequence evolution widens the orbits of massive binaries. This means that systems such as WR20a, DD33J013346.2+304439.9, and the SMC binars almost certainly experienced a phase of mass transfer during their pre-main sequence evolution.

To study how this process will affect massive binaries, we proceed as follows. We assume that a “seed” close protobinary system exists, which may have been formed via one of two possible mechanisms that have been proposed: direct fragmentation of a massive molecular cloud core and subsequent capture of two protostars into a tight binary (e.g. Bonnell & Bate 2005), or fragmentation of a disk around a massive protostar and subsequent migration of a stellar-mass fragment inward (e.g. Kratter & Matzner 2006; Krumholz et al. 2007). Once

*Hubble Fellow

†Lyman Spitzer Jr. Fellow

Electronic address: krumholz@astro.princeton.edu

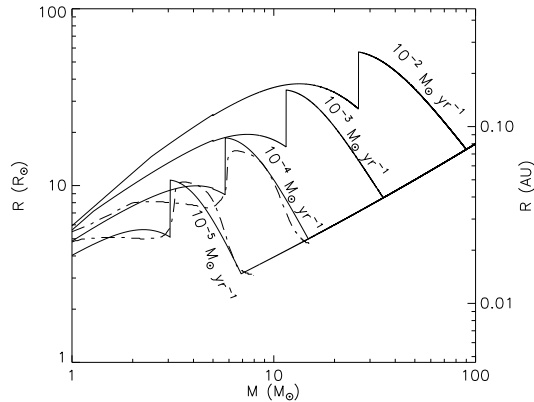


FIG. 1.— Radius versus mass for constant accretion rates of 10^{-5} – $10^{-2} M_{\odot} \text{ yr}^{-1}$ (solid lines), computed using the simple one-zone McKee & Tan (2003) model. For comparison we also show the results of the detailed numerical calculation of Palla & Stahler (1991, 1992) for accretion rates of $10^{-5} M_{\odot} \text{ yr}^{-1}$ and $10^{-4} M_{\odot} \text{ yr}^{-1}$ (dot-dashed line). The sharp rise in R that all models show results from the start of shell deuterium burning.

two protostars are formed into a binary, subsequent accretion may drive them to smaller separations, and bias them toward somewhat larger mass ratios (Bate 2000). We take a binary formed in this manner as a starting point for our calculation of how pre-main sequence stellar evolution and mass transfer may further modify binaries’ properties. In § 2, we determine the range of parameters for which mass transfer can occur, and in § 3 we discuss the outcome of mass transfer when it does occur. We discuss the implications of this process for the massive binary population, and related points, in § 4, and we summarize our conclusions in § 5.

2. THE PROPERTIES OF MASS TRANSFER BINARIES

To determine what types of systems are subject to mass transfer, we adopt a simplified parameter space. We assume that components of a binary system form co-evally or nearly so, limit ourselves to protostars accreting at a constant rate, and to binary systems in circular orbits. In reality, of course, none of these assumptions are likely to be true in detail. Our goal is simply to map out for what ranges of accretion rate and separation mass transfer is a possibility. The first step in exploring this parameter space is to determine the protostellar mass-radius relation as a function of accretion rate, which we do in § 2.1. Using these tracks, in § 2.2 we determine the minimum semi-major axis required for Roche lobe overflow (RLOF) to occur in a binary system consisting of two stars of mass M_1 and M_2 , $M_1 > M_2$, orbiting with semi-major axis a . The total system mass is M , and the binary accretes at a rate \dot{M}_{acc} . Accretion is partitioned between the stars in proportion to their masses, in a ratio $q = \dot{M}_{2,\text{acc}}/\dot{M}_{1,\text{acc}} = M_2/M_1$, where the subscript “acc” indicates the change in mass due to accretion into the system, rather than transfer between the two stars.

2.1. The Protostellar Mass-Radius Relation

For a given accretion rate onto a star we construct a track of radius versus mass using a simple protostellar model. To allow quick exploration of a large range of parameters, we use the one-zone model of McKee & Tan (2003) to generate our tracks. This model has been

calibrated against the detailed numerical calculations of Palla & Stahler (1992), and agrees to $\sim 10\%$. We refer readers to McKee & Tan for a detailed description of the model, but here we summarize its most important features. In this model a protostar is assumed to be a polytropic sphere with a specified accretion rate as a function of time. At every time step of model evolution one uses conservation of energy to determine the new radius, including the effects of energy lost in dissociating and ionizing incoming gas, energy radiated away, and energy gained by Kelvin-Helmoltz contraction, deuterium burning, and the gravitational potential energy of accreting gas.

An accreting massive protostar passes through four distinct phases of evolution before reaching the zero-age main sequence (ZAMS). When the star first forms, it evolves passively without any nuclear burning. When its core becomes hot enough ($\sim 10^6$ K), the second phase begins: deuterium ignites, the star becomes fully convective and begins burning its accumulated deuterium reserve, and contraction of the core temporarily halts. Once the star exhausts its deuterium reserve, it enters a third phase in which it continues burning deuterium at the rate it is brought in by new accretion. Since this is insufficient to maintain hydrostatic balance, the core resumes contracting. As the core temperature continues to rise, its opacity drops, and eventually a layer forms that is stable against convection, initiating the fourth phase. Newly accreted deuterium cannot pass through the radiative layer to reach the core, and the core rapidly exhausts its deuterium supply and becomes convectively stable as well. Deuterium begins burning in a shell above the radiative zone, driving a rapid expansion of the star. As the core continues contracting, the radiative zone increases in size and the star resumes contraction. Eventually the core becomes hot enough to ignite hydrogen, and at that point the star joins the ZAMS.

Figure 1 shows some sample tracks of radius versus mass computed using this model. The sharp increase in radius that each model shows is the result of the start of deuterium shell burning. As the plots show, for the high accretion rates expected in massive star-forming regions, the radius can reach several tenths of an AU. We compute protostellar models for 600 values of \dot{M}_{acc} , uniformly spaced in logarithm in the range 10^{-5} – $10^{-2} M_{\odot} \text{ yr}^{-1}$, accreting up to a maximum mass of $100 M_{\odot}$. By this mass, stars have joined the ZAMS regardless of their accretion rate.

2.2. Roche Lobe Overflow

Having determined the protostellar mass-radius relation, we can now determine for what semi-major axes a a binary of mass ratio q will experience RLOF. The radius of the Roche lobe around star 1 is (Eggleton 1983)

$$R_{r1} \approx a \frac{0.49}{0.6 + q^{2/3} \log(1 + q^{-1/3})}; \quad (1)$$

the Roche lobe radius around star 2 is given by an analogous expression with q replaced by q^{-1} . For a given value of q and $\dot{M}_{1,\text{acc}}$, the accretion rate onto the more massive star, it is straightforward to use the mass-radius tracks to compute whether RLOF ever occurs for a given value of a , and, if so, to determine the mass and state of each star when it does.

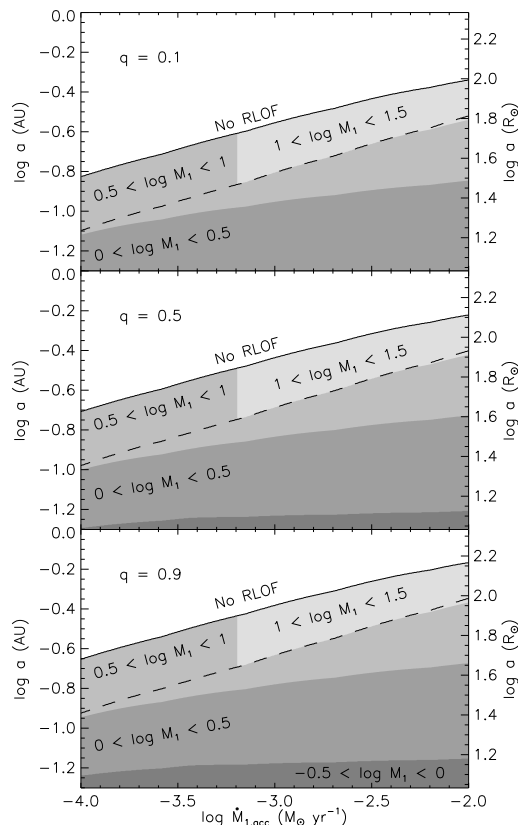


FIG. 2.— Minimum a for RLOF (solid line) as a function of accretion rate onto the more massive star $\dot{M}_{1,\text{acc}}$. The value of q is indicated in each panel. Below the RLOF line, in the region of parameter space where overflow occurs, we show the mass M_1 (in solar units) of the donor star at overflow (shaded regions). Binaries with a below the dashed line experience overflow before the primary starts deuterium shell burning, while those with larger values of a experience overflow after the onset of shell burning.

Figure 2 summarizes the results for 3 different values of q . We find that in rapidly accreting systems, RLOF will occur when the primary star is $M_1 \gtrsim 10 M_\odot$ and the semi-major axis a is a few tenths of an AU or less; a rough analytic estimate for the critical value of a below which RLOF occurs is

$$a_{\text{crit}} \approx 0.2 \dot{M}_{-4}^{1/4} (1+q)^{1/3} \text{ AU}, \quad (2)$$

where $\dot{M}_{-4} = \dot{M}_{1,\text{acc}}/10^{-4} M_\odot \text{ yr}^{-1}$. Observed systems such as WR20a, D33J013346.2+304439.9, and the eclipsing binaries in the SMC, with masses $> 20 M_\odot$ and separations $\lesssim 0.25 \text{ AU}$, are well within the expected overflow range for reasonable accretion rates and initial mass ratios. We further find that it is always the more massive star that overflows its Roche lobe, rather than the less massive one. This is because, despite the larger Roche radius around the more massive star, its higher accretion rate leads this star to have a larger radius before the onset of shell burning, and to start deuterium shell burning sooner. If we were to relax our assumption that the stars are coeval, our conclusion would be strengthened, because simulations indicate that in massive binary systems the more massive companion generally forms earlier (Krumholz et al. 2007). Finally, note that much of the parameter space allowed for transfer, the region between the dashed and solid lines in Figure 2, is due to the shell

burning phase, which roughly doubles the radius of the star and therefore doubles the minimum value of a for which transfer can occur.

3. THE OUTCOME OF ROCHE LOBE OVERFLOW

3.1. Time Scales

Before we attempt to calculate the outcome of RLOF, it is helpful to review some relevant timescales for the problem. The shortest is the orbital period, $P = 3.7a_{0.1}^{3/2} M_{10}^{-1/2}$ days, where $a_{0.1}$ is the semi-major axis in units of 0.1 AU and M_{10} is the total system mass in units of $10 M_\odot$. This is the time scale on which mass lost from the primary star will reach the vicinity of the secondary; actual accretion may take longer if the gas has to be processed through a disk. Next is the dynamical, sound-crossing time of the donor star. The sound speed varies greatly from the stellar core to the surface, so to be conservative and obtain the longest possible time scale we evaluate this using the surface sound speed, which gives $\tau_{\text{dyn}} = R_{*1}/c_{s,\text{surf}} \sim 31 R_{50} T_4^{-1/2}$ days, where R_{50} is the stellar radius in units of $50 R_\odot$ and T_4 is the stellar surface temperature in units of 10^4 K . The timescale τ_{dyn} describes the time required for the star to adjust mechanically as it loses mass. Finally, there is the Kelvin-Helmholtz time of the donor star, $\tau_{\text{KH}} \sim GM_1^2/(R_{*1}L_1) \sim 6200 M_{10}^2 R_{50}^{-1} L_4^{-1} \text{ yr}$, where L_4 is the star's luminosity in units of $10^4 L_\odot$. This describes the time required for the star to adjust thermally to mass loss.

The most important point to take from this calculation is that τ_{KH} is by far the largest timescale in the problem, so that stars will be unable to adjust their thermal (as opposed to mechanical) structure to mass transfer that occurs on orbital or dynamical timescales. Thus, we may approximate stars as behaving adiabatically during mass transfer. A corollary of this is that, as gas in the donor star expands adiabatically in response to mass loss, deuterium burning will slow dramatically, since the burning rate is extremely temperature sensitive. Thus, once the star overflows its Roche lobe, its envelope will not have its specific entropy altered by further nuclear burning on a dynamical time scale.

3.2. Stability of Mass Transfer

We first address the question of whether the RLOF leads to stable or unstable mass transfer. Transfer is stable if adiabatic mass loss shrinks the star at a rate faster than the Roche lobe around it shrinks, and is unstable otherwise. If the transfer is unstable, the donor star can change its mass by order unity on a time scale τ_{dyn} , and transfer will stop only when a new mechanical equilibrium is established.

To check stability, we must evaluate how mass transfer changes both the Roche radius and the stellar radius. The former is easy to compute. If no mass is lost from the system, then conservation of angular momentum demands that the radius of the system shrink at a rate

$$\frac{\dot{a}}{a} = -2 \frac{\dot{M}_1}{M_1} \left(1 - \frac{1}{q_0}\right), \quad (3)$$

where q_0 is the initial mass ratio and \dot{M}_1 is the rate of change of the primary's mass due to mass transfer. Since

$\dot{M}_1 < 0$ and $q_0 < 1$, this means that $\dot{a} < 0$; the semi-major axis of the orbit shrinks in response to mass loss. From equation (1), the Roche radius around the primary star varies approximately as

$$\frac{\dot{R}_{r1}}{R_{r1}} \approx \frac{\dot{M}_1}{M_1} (1 - q_0) \cdot \left[\frac{2}{q_0} + \frac{2 \log(1 + q_0^{-1/3}) - (1 + q_0^{1/3})^{-1}}{1.8 q_0^{1/3} + 3 q_0 \log(1 + q_0^{-1/3})} \right]. \quad (4)$$

The expression in square brackets is always positive for $q_0 < 1$, so the Roche radius around the donor star shrinks as well.

For the range of parameter space we explore, a star undergoing RLOF does so before reaching the ZAMS, and at a mass below $30 M_\odot$. Thus, the star is gas pressure-dominated, at least in its outer layers. If RLOF occurs before the onset of deuterium shell burning, the star is convective throughout, and thus is well-described as an isentropic $n = 3/2$ polytrope. Since a star with this structure expands in response to mass loss at constant entropy (see below), we learn immediately that RLOF will be unstable in this case, because the star expands as the Roche radius contracts. Thus, systems whose parameters fall below the dashed lines in Figure 2 are always unstable.

If RLOF occurs after deuterium shell burning starts, the star consists of a lower specific entropy inner radiative zone and a significantly larger, high specific entropy envelope. Shell burning eventually raises the temperature in the envelope to the point where it becomes radiative as well (Palla & Stahler 1991), but at the onset of shell burning it is still convective. RLOF occurs at the start of shell burning, since this is the point of maximum radius, so the envelope will also be an isentropic $n = 3/2$ polytrope, with a different specific entropy than the interior radiative zone.

Following the analysis of Paczyński & Sienkiewicz (1972) for a red giant, we can approximate this configuration in terms of a “centrally condensed” polytrope, a polytropic sphere with a point mass in its center. This is a less accurate approximation than it is for a red giant, since deuterium shell burning in a protostar only expands the envelope by a factor of slightly more than 2, as opposed to more than an order of magnitude for a red giant. However, we can regard the pure polytropic model of a star before shell burning and the centrally condensed polytropic model for a star during shell burning as limiting cases.

Centrally condensed $n = 3/2$ polytropes obey a mass-radius relation (Paczyński & Sienkiewicz 1972)

$$R = K E^{2/3} M^{-1/3}, \quad (5)$$

where K is a constant that depends on the specific entropy in the convective envelope and E is a dimensionless number that depends only on ξ , the ratio of the core mass to the total mass. Since the star behaves adiabatically as mass is removed, K remains constant. If the mass of the radiative core is also unchanged, a reasonable approximation when transfer begins, then the radius of the star varies as

$$\frac{\dot{R}_{*1}}{R_{*1}} = -\frac{\dot{M}_1}{3M_1} \left\{ 1 + 2 \left[\frac{\xi_0}{E(\xi_0)} \right] \frac{dE}{d\xi} \bigg|_{\xi=\xi_0} \right\}, \quad (6)$$

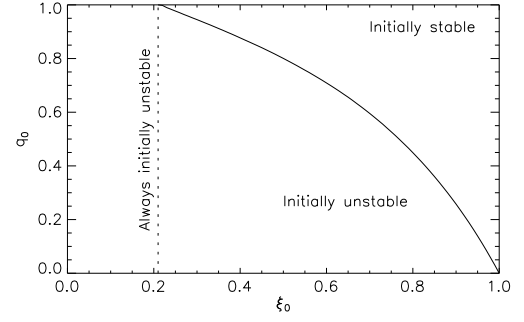


FIG. 3.— Minimum initial mass ratio q_0 required to make mass transfer stable for a given initial core mass fraction ξ_0 . The dotted line at $\xi_0 = 0.22$ indicates the minimum ξ_0 below which mass transfer is always unstable regardless of the value of q_0 .

where ξ_0 is the core mass ratio at the start of mass loss. The star expands for $\xi_0 < 0.22$, and shrinks for $\xi_0 > 0.22$.

Since $R_{r1} = R_{*1}$ at the start of mass loss, mass transfer is unstable unless $\dot{R}_{*1} < \dot{R}_{r1}$. This condition is met only if

$$\frac{1}{3} \left\{ 1 + 2 \left[\frac{\xi_0}{E(\xi_0)} \right] \frac{dE}{d\xi} \bigg|_{\xi=\xi_0} \right\} < (1 - q_0) \left[\frac{2}{q_0} + \frac{2 \log(1 + q_0^{-1/3}) - (1 + q_0^{1/3})^{-1}}{1.8 q_0^{1/3} + 3 q_0 \log(1 + q_0^{-1/3})} \right]. \quad (7)$$

By evaluating E and $dE/d\xi$ numerically (e.g. table 1 of Paczyński & Sienkiewicz 1972), this condition lets us identify for each ξ_0 what values of the initial mass ratio q_0 produce stability. Figure 3 shows that for $\xi_0 < 0.22$ no stability is possible because the star expands rather than contracting in response to mass loss.

Stars without radiative cores have $\xi = 0$, so if RLOF occurs before the onset of shell burning then $\xi_0 = 0$ and the transfer is unstable. Shell burning stars will have $\xi_0 > 0$, and they may be stable if ξ_0 and q_0 are large enough. RLOF is likely to be initiated just after the start of shell burning, since this is the time when the star achieves its maximum radius. The value of ξ_0 at this time is determined by the radius of the shell where the maximum luminosity that can be transported by radiation, $L_{\text{rad}}(m)$, first rises to the point where it is equal to the luminosity passing through that shell, $L(m)$. Here, m is the mass enclosed within a given shell, and varies from $m = 0$ at the center of the star to $m = M_1$ at its surface.

From their numerical models, Palla & Stahler (1992) find that $L_{\text{rad}}(m) = L(m)$ is first satisfied at $m/M_1 = \xi_0 = 0.20, 0.21$, and 0.41 for accretion rates of 10^{-5} , 3×10^{-5} , and $10^{-4} M_\odot \text{ yr}^{-1}$. We would like to extrapolate to higher accretion rates, but that is quite difficult because ξ_0 varies so non-linearly with $\dot{M}_{1,\text{acc}}$. Instead, we make some general observations to help understand the likely value of ξ_0 . The non-linearity in the variation of ξ_0 with $\dot{M}_{1,\text{acc}}$ results from the complicated shape of $L_{\text{rad}}(m)$ (see figure 5 of Palla & Stahler 1991). This shape admits two possible solutions to $L_{\text{rad}}(m) = L(m)$, i.e. two mass shells where a convectively stable zone could appear, one at smaller m and one at larger m . The reason ξ_0 is nearly unchanged between $\dot{M}_{1,\text{acc}} = 10^{-5}$ and $3 \times 10^{-5} M_\odot \text{ yr}^{-1}$ is that $L_{\text{rad}}(m) = L(m)$ is first sat-

ified at the same solution point in the two models; ξ_0 jumps between $\dot{M}_{1,\text{acc}} = 3 \times 10^{-5}$ and $10^{-4} M_\odot \text{ yr}^{-1}$ because the point where $L_{\text{rad}}(m)$ and $L(m)$ first become equal moves from the inner to the outer possible solution. Since the shape of the $L_{\text{rad}}(m)$ curve does not suggest that there are other, larger mass solutions where $L_{\text{rad}}(m) = L(m)$ might first occur, it seems unlikely that ξ_0 will be much larger than 0.41. However, we caution that this is a tentative conclusion, and that one cannot confidently estimate ξ_0 without detailed numerical modeling. In particular, the value of ξ_0 in the models of Palla & Stahler (1991, 1992) appears to be sensitive to their choice of boundary condition.

If our tentative conclusion holds and $\xi_0 \lesssim 0.5$ regardless of the accretion rate, then transfer will be unstable unless $q_0 \gtrsim 0.8$.

3.3. Termination of Mass Transfer

We have found that unless the mass ratio is already near unity and the donor star is shell burning, mass transfer is unstable and proceeds on a dynamical time scale. This makes it difficult to determine the precise outcome without a protostellar model that, unlike ours, is capable of following the accretion of very high entropy gas on this time scale. Numerical simulations of the transfer itself would also be helpful, since in the case of runaway transfer it is possible that mass lost from the primary may go into a circumbinary disk or a wind rather than accreting onto the secondary. Nonetheless, we can make some simple calculations to estimate how and whether mass transfer will cease.

Mass transfer will continue until either the primary shrinks within its Roche lobe, or until the secondary overflows its Roche lobe too. We discuss the latter outcome in § 3.4. We can check whether the former is a possibility by asking whether there exists a new mass ratio q , larger than the original mass ratio q_0 , such that the primary is again within its Roche lobe. Since such an equilibrium must be established on the dynamical time scale, the donor star must be able to reach it adiabatically. To determine whether such an equilibrium exists, we first examine how the Roche radius and stellar radius change with q in § 3.3.1, and then we search for equilibria in § 3.3.2.

3.3.1. Roche Radius and Stellar Radius

If the mass transfer conserves both total system mass and angular momentum, then the ratio of the semi-major axis to its value before transfer starts is

$$\frac{a}{a_0} = \left(\frac{q_0}{q}\right)^2 \left(\frac{1+q}{1+q_0}\right)^4 \quad (8)$$

when the mass ratio reaches q . From equation (1), the new Roche radius of the primary is related to the original one $R_{r1,0}$ by

$$\frac{R_{r1}}{R_{r1,0}} = \left(\frac{q_0}{q}\right)^2 \left(\frac{1+q}{1+q_0}\right)^4 \left[\frac{0.6 + q_0^{2/3} \log(1 + q_0^{-1/3})}{0.6 + q^{2/3} \log(1 + q^{-1/3})} \right]. \quad (9)$$

Similarly, from the mass-radius relation (5), the initial stellar radius and that predicted by our centrally-

condensed polytrope (ccp) model are related by

$$\frac{R_{\text{ccp}}}{R_{*1,0}} = \left(\frac{1+q}{1+q_0}\right)^{1/3} \left[\frac{E\left(\frac{1+q}{1+q_0} \xi_0\right)}{E(\xi_0)} \right]^{2/3}. \quad (10)$$

This relation will break down if $\xi = \xi_0(1+q)/(1+q_0)$ becomes too large, because formally a centrally condensed polytrope goes to zero radius as $\xi \rightarrow 1$. In reality, the radiative core has a finite radius, which the simulations of Palla & Stahler (1991, 1992) show is $\sim 1/2$ of a dex smaller than the total stellar radius at the onset of shell burning.

We thus require a mass-radius relation for the central radiative core as the mass of the overlying convective envelope decreases due to RLOF. The stellar radius cannot be smaller than the core radius, R_{co} , because the core is a pure polytrope and will expand if it loses mass. Thus, $R_* = R_{\text{co}}$ is the minimum size for which the star can be in equilibrium while behaving adiabatically. We construct an approximate mass-radius relation for the star as it loses mass by assuming that, as long as the stellar radius R_{ccp} for a centrally condensed polytrope is larger than the core radius R_{co} , the stellar radius $R_{*1} = R_{\text{ccp}}$. However, if q reaches the point where $R_{\text{ccp}} = R_{\text{co}}$ without the donor star shrinking within its Roche lobe, the envelope will be gone completely, and it will be impossible for the binary to establish a new equilibrium.

We consider two limiting cases for R_{co} as the mass of the convective envelope (M_{env}) decreases. First, if the mass of the envelope is very small with respect to the core, then we may simply approximate R_{co} as fixed, for a given core mass, as M_{env} decreases. In this case, we take

$$R_{\text{co}} = R_{\text{co},0} = R_{*1,0}/10^{1/2}. \quad (11)$$

At the opposite extreme, we consider a very massive envelope for which the self-gravitational binding energy of the envelope is much greater than either the self-gravitational binding energy of the core or the binding energy of the core with the envelope. In this case the pressure P_{env} at the base of the envelope is entirely due to the self-gravity of the envelope, and varies with mass as $P_{\text{env}} \propto M_{\text{env}}^{10/3}$, the normal relation for an $n = 3/2$ polytrope. Since the binding energy of the core is negligible in comparison to that of the envelope, the core's gravity contributes no additional pressure, and the pressure within the core is $P_{\text{co}} \approx P_{\text{env}}$. Since the core is a polytrope as well, $P_{\text{co}} \propto R_{\text{co}}^{-3(1+1/n_{\text{co}})}$, where n_{co} is the polytropic index of the core. Although the core is radiative, at the start of shell burning it has just become so, and it is likely still close to isentropic. We therefore take $n_{\text{co}} = 3/2$, giving $R_{\text{co}} \propto M_{\text{env}}^{-2/3}$. The expression for the evolution of R_{co} as the primary envelope is accreted onto the secondary is then

$$\frac{R_{\text{co}}}{R_{\text{co},0}} = \left(\frac{M_{\text{env},0}}{M_{\text{env}}}\right)^{2/3} = \left[\left(\frac{1+q_0}{1+q}\right) \left(\frac{1-\xi}{1-\xi_0}\right) \right]^{2/3}, \quad (12)$$

where $\xi = \xi_0(1+q)/(1+q_0)$ and $R_{\text{co},0} = R_{*1,0}/10^{1/2}$. Although these two limiting cases (eqs. 11 & 12) are each uncertain and merely approximate, they serve to delineate the importance of finite core size as the system adjusts during RLOF of the primary.

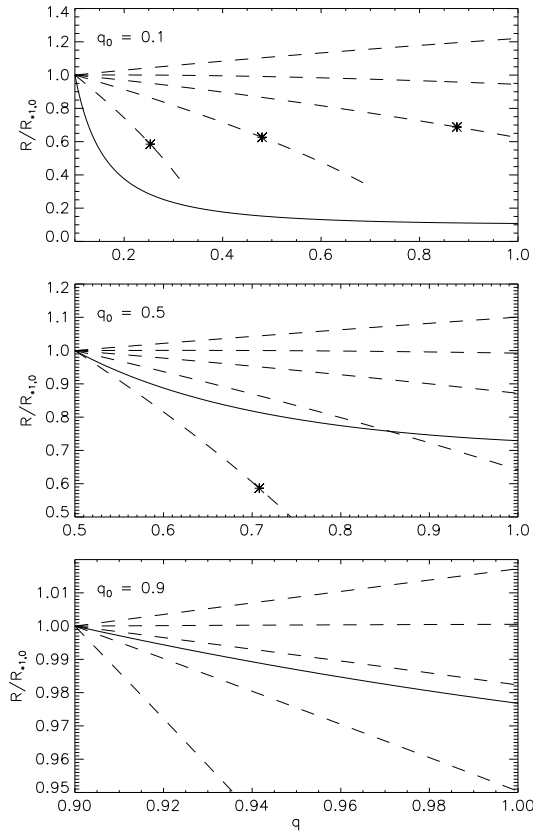


FIG. 4.— Roche radius (solid line) and stellar radii for $\xi_0 = 0, 0.2, 0.4, 0.6$, and 0.8 (dashed lines, highest to lowest), normalized to initial radius. The plot for $q_0 = 0.1$ cuts off at $q = 0.21$ because that is the value of q for which $R_{\text{ccp}} = R_{\text{co}}$. Asterisks mark the point where $R_{*1} = R_{\text{co}}$ as estimated from equation 12, and the dashed lines terminate when $R_{*1} = R_{\text{co}} = R_{*1,0}/10^{1/2}$ as estimated from equation 11.

Before moving on, we emphasize that one major approximation of this treatment of the star is our assumption that the radiative core stays adiabatic. In reality, as it expands, its opacity will increase and it may transition back to convective instability. If this happens, it will start mixing with the convective envelope on top of it and attempt to establish a zero entropy gradient. However, the time to establish this is at least the dynamical time scale of the star, which is also the mass time scale. Thus, our approximation that both the envelope and the core material remain adiabatic is probably reasonable.

3.3.2. Existence of Mechanical Equilibria

Having determined how the Roche radius and stellar radius vary as the primary loses mass and q changes, we are now in a position to determine whether there is a state the primary can reach adiabatically in which it is no longer overflowing its Roche lobe. Such a configuration exists only if there is a value of q , larger than q_0 and smaller than the value of q for which $R_{*1} = R_{\text{ccp}} = R_{\text{co}}$, such that $R_{r1} = R_{*1}$. We also require $q < 1$ for reasons we discuss below.

We plot the problem graphically in Figure 4, which shows the Roche radius and stellar radius as a function of q for various values of q_0 and ξ_0 . For a given initial mass ratio q_0 and core mass ratio ξ_0 , there may or may not be a value of $q > q_0$ such that $R_{r1} = R_{*1}$. Asterisks

denote the points at which the stellar radius reaches R_{co} as defined in equation (12), whereas the dashed lines terminate at the point where $R_{*1} = R_{\text{co}} = R_{*1,0}/10^{1/2}$ as defined estimated in equation 11. In some cases, as in all of the curves in the top panel of Figure 4 for $q_0 = 0.1$, the Roche radius R_{r1} shrinks to become smaller than the minimum stellar radius R_{co} before the star reaches that radius, and there is no solution to $R_{r1} = R_{*1}$. For these cases, the star can never shrink within its Roche lobe, and mass transfer will continue indefinitely. However, for other sets of parameters solutions do exist and the system can stabilize by evolving to higher q . For example, the middle panel of Figure 4 shows that for $q_0 = 0.5$ and $\xi_0 = 0.6$, the system achieves stability at $q \approx 0.85$, but for $\xi_0 = 0.4$ no solution exists and the system cannot reach equilibrium.

We summarize these results in Figure 5, which shows the value of q for which a system stabilizes as a function of q_0 and ξ_0 . In the upper right white region of the plot, systems are initially stable and mass transfer does not occur on a dynamical time scale. In the lower left region, systems are always unstable, and there is no value of q for which the donor star can shrink within its Roche lobe. Systems whose parameters fall within the shaded region in between are initially unstable, but can stabilize and stop transferring mass for some value of q between q_0 and 1. The full shaded region — including the cross-hatched area — shows our results for the case holding R_{co} constant during mass transfer (eq. 11). The other limiting case with R_{co} given by equation (12) is more restrictive because the core radius increases in size as the envelope mass decreases during RLOF. For this reason, the island of stability is smaller, and systems whose values of q_0 and ξ_0 fall within the cross-hatched area are unstable. Generically, we find that for $\xi_0 \lesssim 0.5$, the system is unstable. Thus, RLOF in systems accreting at relatively modest rates of a few $10^{-4} M_{\odot} \text{ yr}^{-1}$ or less cannot reach stability. For higher accretion rates the results of Palla & Stahler (1992) suggest that ξ_0 will still be $\lesssim 0.5$, and again stability will not be possible unless q_0 is fairly large before mass transfer starts. For larger ξ_0 and $q_0 \gtrsim 0.2$, stable solutions can be found with q significantly less than unity, depending on the evolution of $R_{\text{co}}(M_{\text{env}})$ during RLOF.

3.4. The Fate of Unstable Mass Transfer Binaries

What is the fate of primary stars that cannot stop mass transfer by shrinking inside their Roche lobes? For these stars, the likely end to mass transfer is growth of the secondary. Material transferred from the primary to the secondary will retain its specific entropy, which at the onset of mass transfer is larger than the specific entropy in the envelope of the secondary. This is due to the primary's higher mass and accretion rate, and, if it has started, to shell burning. Thus, when gas from the primary accretes onto the secondary, initially it will be stable against convection. It will not mix and reach the same entropy as the rest of the secondary until it cools radiatively, on a Kelvin-Helmholtz time scale.

The radius of the star is determined largely by the specific entropy of the gas in its outer layers. Since the newly accreted mass has the same specific entropy as before its transfer, and it is now bound to a less massive

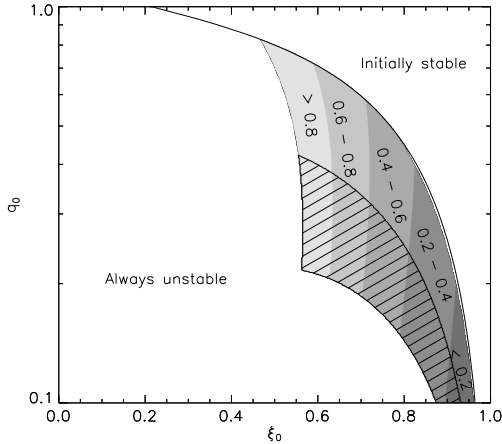


FIG. 5.— Value of q for which mass transfer terminates, as a function of ξ_0 and q_0 . Outside the shaded region, mass transfer is either always stable (*top right region*), or there is no value of q for which it will terminate (*bottom left region*). Inside the shaded region, we show the value of q for which $R_{r1} = R_{*1}$ and mass transfer terminates. The full shaded region including the cross-hatched area corresponds to the limiting case for the evolution of R_{co} given in equation (11), whereas the smaller shaded region without the cross-hatched area denotes stability for the case where R_{co} is given by equation (12).

star than before the transfer, the resulting radius is likely to be larger. Thus, if the primary overflows its Roche lobe and transfers a substantial fraction of its mass, the material transferred to the secondary is likely to result in RLOF for it as well. Then both stars will fill their Roche lobes, and the system will become a contact binary, or possibly even a common envelope system if the semi-major axis decreases enough. Equation (8) implies that in a binary that transfers enough mass to reach $q = 1$, the semi-major axis shrinks by a factor of $2^4 q_0^2 / (1 + q_0)^4$. For $q_0 = 0.1$, this is a factor of 10, and almost certainly produces common envelope evolution, or possibly even a merger. However, for $q_0 = 0.5$, the change in separation is only 20%.

Formation of a contact binary or a common envelope system will definitely halt mass transfer before the system reaches $q = 1$, which is why we only searched for new equilibria in that region in § 3.3.2. Systems that undergo rapid mass transfer but are able to stabilize at $q < 1$, i.e. those in the shaded region of Figure 5, may also become contact binaries before reaching their equilibrium values of q , since double overflow may happen a bit before $q = 1$. Thus, we expect contact binaries to be a fairly common result of RLOF.

Once mass transfer stops, over a thermal time the envelopes of stars in a contact binary will equilibrate to the same specific entropy. If the primary has a radiative core it will not equilibrate, but the radiative core may well disappear temporarily because as it expands and cools adiabatically, its opacity will increase, and it may transition back to convective instability. If this happens, it will reach the same specific entropy as the two envelopes. The result will be an isentropic contact binary with a mass ratio near unity. As the stars radiate they will continue contracting, their envelopes will shrink, and eventually contact will cease before the stars reach the ZAMS. The result will be a main sequence detached binary with a mass ratio close to unity.

4. DISCUSSION

A primary result of this work is that there is a critical a below which RLOF occurs (eq. 2; Figure 2). Thus, for massive binaries that form at a separation of a few tenths of an AU, RLOF and mass transfer occur before either star reaches the ZAMS. For a relatively wide range of parameter space, mass transfer is unstable and we argue that the binary mass ratio will be driven toward equality on a dynamical timescale. For high system accretion rates, the ratio of the radiative core mass to the envelope mass of the primary protostar (ξ_0) can be ~ 0.5 , and the system can be stabilize for some values of $q < 1$. Somewhat unequal mass binaries are the result when the stars reach the ZAMS (Figure 5).

4.1. “Twin” Binaries

A particularly curious feature of the massive binary population is the high proportion of systems with mass ratios very close to unity. The mass ratio of WR20a is $q = 0.99 \pm 0.05$ (Bonanos et al. 2004; Rauw et al. 2005), and that of D33J013346.2+304439.9 is $q = 0.90 \pm 0.15$ (Bonanos et al. 2006). Thirteen of the 21 detached binaries in the Hilditch et al. (2005) sample have $q > 0.85$, and five have best fit values of q consistent with $q = 1.0$ (Pinsonneault & Stanek 2006). Due to its small size, the statistical significance of this sample is unclear (Lucy 2006), but a priori it seems quite unusual that almost 25% of the eclipsing binaries in the SMC with orbital periods shorter than 5 days should have mass ratios consistent with 1.0. Nor does it seem likely a priori that the most massive binary known should have a mass ratio within 5% of unity.

Accretion from a circumbinary disk does provide a way of producing an anti-correlation between semi-major axis and mass ratio (Bate 2000), such as is observed even for low mass stars (Tokovinin 2000). However, it does not provide a mechanism for making true twins, systems like WR20a whose mass ratios are almost unity. Indeed, how much mass from a circumbinary disk accretes onto each stellar component probably depends on a complex magnetic field geometry connecting the disk and the stars, an effect not included by Bate. It is hard to see why this would favor $q = 1.0$. On the other hand, mass transfer between accreting protostars does provide a natural, and for close binaries inevitable, mechanism to reach mass ratios near unity. The circumbinary accretion mechanism of Bate may operate in tandem with mass transfer, bringing binaries closer together and pushing mass ratios to larger values, before mass transfer occurs and produces q of nearly 1.0.

4.2. Observational Predictions

These calculations lead to definite predictions about the properties of massive binaries, which will be directly testable against future larger than those available today. Since there is both a critical mass and a critical semi-major axis required for RLOF to occur, we predict that true twins, systems with mass ratios $q > 0.95$, should be significantly more common among stars with masses $\gtrsim 5 - 10 M_\odot$ with semi-major axes $\lesssim 0.25$ AU than among a binary population with either lower mass or larger separation. These twins should be in nearly zero eccentricity orbits, since mass transfer and evolution into

a contact binary will circularize orbits rapidly.

Massive stars should generally have larger mass ratios in clusters with high surface density, since these likely formed from higher pressure gas and thus produced larger accretion rates onto the stars within them (McKee & Tan 2003). However, this effect is likely to be rather weak, since the critical semi-major axis only varies with the quarter power of accretion rate, and very high accretion rates make it easier for stars to remain unequal mass after the onset of transfer because they decrease the fraction of the star's mass that goes into the extended envelope. As a result, there may be fewer true twins in very high surface density systems, even if there are more massive stars with mass ratios $\gtrsim 0.5$. In any event, due to weak dependence on the accretion rate, we consider this possibility less promising than searching for correlations of twin fraction with mass and semi-major axis.

4.3. Primordial Stars

One final note is that, although we have not discussed primordial stars, the mechanism we have discussed may well operate in them too. The critical ingredients for mass transfer are a phase of deuterium shell burning to produce large radii, and a close companion onto which to transfer mass. The binary properties of primordial stars are completely unknown, so we cannot comment on whether the second condition is likely to be met. However, a phase of deuterium shell burning does seem likely. Primordial stars probably form at high accretion rates (Tan & McKee 2004), giving them large radii. In present-day stars, a radiative barrier forms because opacity in a stellar interior decreases with temperature. The opacity source is primarily free-free transitions of electrons, and the availability of electrons for this process does not depend strongly on metallicity in an ionized stellar interior. Thus, primordial stars likely form radiative barriers much like present day ones, and undergo deuterium shell burning.

5. SUMMARY

Massive, rapidly accreting protostars can reach radii of tenths of an AU during their pre-main sequence evolution, largely because they undergo a phase of deuterium shell burning that swells their radii. During this evolutionary phase, massive protostars with close companions will overflow their Roche lobes and transfer mass. Such transfer is always from the more massive, rapidly accreting star to the smaller one, since radius increases with both mass and accretion rate. Using simple protostellar

structure and evolution models, we evaluate the range of separations and mass ratios for which mass transfer is expected to occur, and compute the likely outcome of the transfer.

We find that, for the expected accretion rates in mass star-forming regions, binaries at separations of several tenths of an AU or closer will undergo mass transfer, with some dependence on the exact accretion rate and the initial mass ratio. This process always pushes binaries toward mass ratios of unity. For some accretion rates and initial mass ratios, mass transfer will either be stable initially, or will terminate on its own before reaching $q = 1$. For many systems, though, it will only halt when the two stars form a contact binary. The stellar envelopes in such systems will rapidly reach almost equal masses and specific entropies, and then the stars contract onto the main sequence, forming a ZAMS binary with a mass ratio very close to unity.

Pre-main sequence mass transfer represents a heretofore unknown phase of binary star formation and evolution, one that has likely affected a significant fraction of massive spectroscopic binaries. It provides a natural explanation for the puzzling phenomenon of massive twins, high mass binaries with mass ratios that are consistent with $q = 1.0$. We predict based on this finding that twins should be significantly more common among stars $\gtrsim 5\text{--}10 M_{\odot}$ in mass at separations $\lesssim 0.25$ AU than among either less massive or more distant stars, and that mass ratios should generally increase with binary mass and decrease with separation. The weak dependence of a_{crit} in equation (2) on the system mass accretion rate and the initial mass ratio suggests that this result should not depend significantly on formation environment. Surveys such as OGLE that detect statistically large samples of massive binaries are rapidly making these predictions testable.

We thank J. Goodman and S. Stahler for helpful discussions, J. M. Stone for discussions and for a careful reading of the manuscript, and B. Paczyński for prompting us to think about this problem. MRK acknowledges support from NASA through Hubble Fellowship grant #HSF-HF-01186 awarded by the Space Telescope Science Institute, which is operated by the Association of Universities for Research in Astronomy, Inc., for NASA, under contract NAS 5-26555. TAT acknowledges support from a Lyman Spitzer, Jr. Fellowship.

REFERENCES

- Bate, M. R. 2000, *MNRAS*, 314, 33
 Bonanos, A. Z., Stanek, K. Z., Kudritzki, R. P., Macri, L., Sasselov, D. D., Kaluzny, J., Stetson, P. B., Bersier, D., Bresolin, F., Matheson, T., Mochejska, B. J., Przybilla, N., Szentgyorgyi, A. H., Tonry, J., & Torres, G. 2006, *ApJ*, 652, 313
 Bonanos, A. Z., Stanek, K. Z., Udalski, A., Wyrzykowski, L., Żebruń, K., Kubiak, M., Szymański, M. K., Szewczyk, O., Pietrzyński, G., & Soszyński, I. 2004, *ApJ*, 611, L33
 Bonnell, I. A. & Bate, M. R. 2005, *MNRAS*, 362, 915
 Eggleton, P. P. 1983, *ApJ*, 268, 368
 Harries, T. J., Hilditch, R. W., & Howarth, I. D. 2003, *MNRAS*, 339, 157
 Henning, T., Schreyer, K., Launhardt, R., & Burkert, A. 2000, *A&A*, 353, 211
 Hilditch, R. W., Howarth, I. D., & Harries, T. J. 2005, *MNRAS*, 357, 304
 Kratter, K. M. & Matzner, C. D. 2006, *MNRAS*, in press, astro-ph/0609692
 Krumholz, M. R. 2006, *ApJ*, 641, L45
 Krumholz, M. R., Klein, R. I., & McKee, C. F. 2007, *ApJ*, in press, astro-ph/0609798
 Lada, C. J. 2006, *ApJ*, 640, L63
 Lucy, L. B. 2006, *A&A*, 457, 629
 McKee, C. F. & Tan, J. C. 2003, *ApJ*, 585, 850
 Paczyński, B. & Sienkiewicz, R. 1972, *Acta Astronomica*, 22, 73
 Palla, F. & Stahler, S. W. 1991, *ApJ*, 375, 288
 —. 1992, *ApJ*, 392, 667
 Pinsonneault, M. H. & Stanek, K. Z. 2006, *ApJ*, 639, L67

- Preibisch, T., Weigelt, G., & Zinnecker, H. 2001, in IAU Symposium, ed. H. Zinnecker & R. Mathieu, 69—
- Rauw, G., Crowther, P. A., De Becker, M., Gosset, E., Nazé, Y., Sana, H., van der Hucht, K. A., Vreux, J.-M., & Williams, P. M. 2005, *A&A*, 432, 985
- Shatsky, N. & Tokovinin, A. 2002, *A&A*, 382, 92
- Stahler, S. W. 1988, *ApJ*, 332, 804
- Tan, J. C. & McKee, C. F. 2004, *ApJ*, 603, 383
- Tokovinin, A. A. 2000, *A&A*, 360, 997
- Udalski, A., Soszynski, I., Szymanski, M., Kubiak, M., Pietrzynski, G., Wozniak, P., & Zebrun, K. 1998, *Acta Astronomica*, 48, 563